NANO LETTERS

pubs.acs.org/NanoLett Letter

Enhancing Biohybrid CO_2 to Multicarbon Reduction via Adapted Whole-Cell Catalysts

Jimin Kim, Stefano Cestellos-Blanco, Yue-xiao Shen, Rong Cai, and Peidong Yang*

Cite This: https://doi.org/10.1021/acs.nanolett.2c01576 Read Online

ACCESS | Metrics & More | Article Recommendations | Supporting Information

ABSTRACT: Catalytic CO_2 conversion to renewable fuel is of utmost importance to establish a carbon-neutral society. Bioelectrochemical CO_2 reduction, in which a solid cathode interfaces with CO_2-reducing bacteria, represents a promising approach for renewable and sustainable fuel production. The rational design of biocatalysts in the biohybrid system is imperative to effectively reduce CO_2 into valuable chemicals. Here, we introduce methanol adapted *Sporomusa ovata* (*S. ovata*) to enhance the slow metabolic activity of wild-type microorganisms to our semiconductive silicon nanowires (Si NWs) array for efficient CO_2 reduction. The adapted whole-cell catalysts enable an enhancement of CO_2 fixation with a superior faradaic efficiency on the poised Si NWs cathode. The synergy of the high-surface-area cathode and the adapted strain achieves a CO_2-reducing current density of 0.88 ± 0.11 mA/cm^2, which is 2.4-fold higher than the wild-type strain. This new generation of biohybrids using adapted *S. ovata* also decreases the charge transfer resistance at the cathodic interface and facilitates the faster charge transfer from the solid electrode to bacteria.

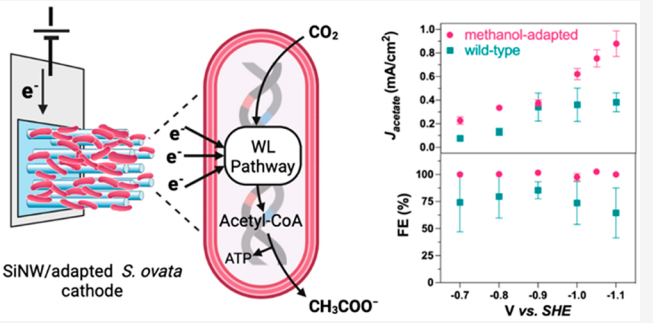

KEYWORDS: *CO_2 reduction, Si nanowires, biocatalysis, bacteria, bioelectrochemical, bionano interface*

Electrochemical CO_2 reduction represents a promising way to convert CO_2 into chemical feedstocks and store electricity in the form of chemical bonds.[1−3] However, current systems still suffer from low selectivity, activity, and stability.[4,5] Catalyst design is one of the keys to addressing these challenges. Nature's catalytic machinery provides a prime example of such catalysts with its efficient and selective cascade reactions.[6] Acetogens can selectively convert CO_2 to acetate by the Wood−Ljungdahl pathway (WLP), which is the most energetically efficient CO_2-fixation pathway.[7,8] Some of the microbes that encode the WLP can perform extracellular electron uptake to transfer electrons from electrodes, which makes them attractive electrocatalysts.[9−14] Particularly, Liu et al. first introduced a biohybrid of silicon (Si) nanowire photocathode and acetogen *Sporomusa ovata* (*S. ovata*) that allowed for unassisted solar-to-chemical production at a low overpotential of 200 mV and a high Faradaic efficiency up to 90%.[15] The high surface area of Si nanowires enables the high interfacial area between bacteria and the electrodes. Su et al. further optimized electrode potential, electrolyte pH, and biocatalyst loading of the system to maximize the interfacial area between living cells and cathodes. Because of the increased direct attachment of catalysts to the electrodes, these "close-packed" bacteria/nanowire hybrids reach 3.6% solar-to-chemical conversion efficiency.[16]

However, the CO_2-reduction rates of biocatalysts systems are still low compared to those of abiotic electrochemical systems such as with copper electrocatalysts being at least one or two orders of magnitude higher in terms of producing C_2 products (>100 mA/cm^2).[17−19] A crucial rate-limiting step in biohybrid systems for chemical production is the CO_2 fixation rate of individual bacteria.[20−22] Adaptative laboratory evolution (ALE) offers a method to metabolically engineer microorganisms, especially for those lacking genetic engineering tools.[23−25] Tremblay et al. demonstrated that ALE of *S. ovata* using methanol, a toxic C_1 compound, as the sole electron donor accelerates the autotrophic metabolism of *S. ovata*.[23] Their adapted strain showed a 0.2 mA/cm^2 of CO_2-reduction rate on the graphite cathode, which was 6.8-fold higher than the wild-type strain. Thus, ALE offers one route to improve the rate of CO_2 fixation and the overall efficiency of our close-packed biohybrid system.

In this study, we enhanced the CO_2-reduction rate of our model *S. ovata*/silicon nanowire hybrid platform by introducing a robust methanol adapted *S. ovata* strain as the biocatalyst. First, we conducted methanol adaptation of *S. ovata* by the

Received: April 23, 2022
Revised: June 13, 2022

https://doi.org/10.1021/acs.nanolett.2c01576
Nano Lett. XXXX, XXX, XXX−XXX

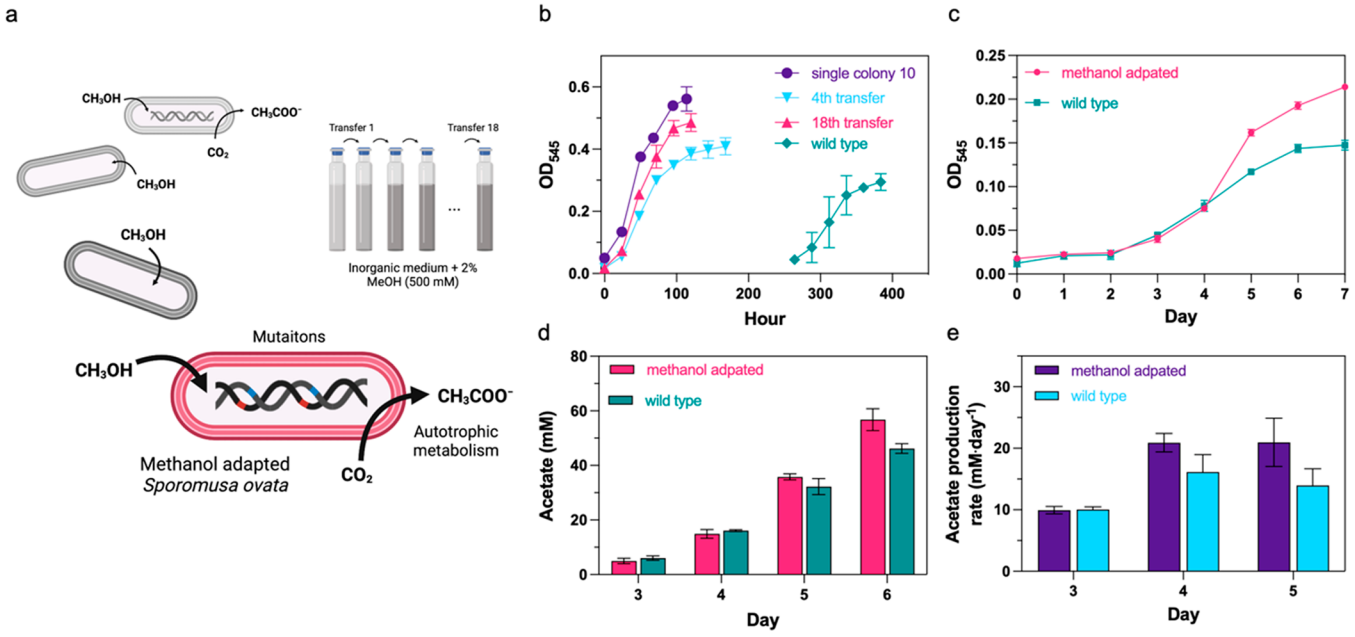

Figure 1. Methanol adaptation of WT *S. ovata* through the ALE process and the phenotypical enhancements of autotrophic growth of the methanol adapted *S. ovata*. (a) Illustration of the adaptive laboratory evolution process with 2% methanol containing inorganic medium and 10% v/v bacteria inoculation under strict anaerobic conditions (80% N_2/20% CO_2) (see methods in Supporting Information). Toxic methanol is used as a growth substrate during the ALE process, and the genetic mutations are accumulated to enhance the autotrophic metabolism of *S. ovata* through the end of ALE. (b) Growth curves using 2% methanol of WT *S. ovata*, 4th transfer, 18th transfers, and an isolated clone from the 18th transfer cultures. (c) Growth curves of the methanol adapted and WT *S. ovata* under hydrogen. The faster growth rates of methanol adapted *S. ovata* compared to WT strain demonstrates that the methanol adapted *S. ovata* exhibits enhanced autotrophic growth using methanol and hydrogen. (d) Acetate production and (e) acetate production rate of the methanol adapted *S. ovata* and WT *S. ovata* using hydrogen during the exponential growth period (day 3−day 6). All error bars represent the mean ± s.d. (n = 3 biological independent samples).

ALE method introduced by Tremblay et al. We observed an enhanced autotrophic metabolic activity under methanol and hydrogen (H_2)/CO_2, respectively. We sequenced the genomes of the wild-type (WT) and our adapted strain and found multiple mutations in key enzymes of WLP. The methanol adaptation of *S. ovata* successfully boosted the CO_2-reducing current density on the nanowire cathode. In our model, close-packed biohybrid system with the methanol adapted *S. ovata* achieved the highest CO_2-reducing current density ($J_{acetate}$) of 0.88 ± 0.11 mA cm^{-2} at −1.1 V versus standard hydrogen electrode (*SHE*), with a superior faradaic efficiency of acetate ($FE_{acetate}$) of close to 100%. Compared to the previous study of Tremblay et al., our close-packed system with the adapted *S. ovata* achieved a 4.4-fold higher CO_2-reduction rate on the high surface area of Si NWs at the optimal electrolyte pH, biocatalyst loading, and applied overpotential. Furthermore, electrochemical impedance spectroscopy (EIS) was utilized to elucidate the charge transfer kinetics of the bacteria/cathode interface. The adapted *S. ovata*/Si nanowire interface exhibits lower charge transfer resistance in comparison to the WT *S. ovata*/Si nanowire interface.

Methanol Adaptation of *Sporomusa ovata*. Methanol adaptation of *S. ovata* was carried out by the ALE method reported by Tremblay et al.[23] WT *S. ovata* was inoculated in the autotrophic medium with 2% v/v methanol as the sole electron donor, and the methanol-grown *S. ovata* was propagated in the same medium for 18 transfers (Figure 1a). After the 18th transfer, equivalent to ∼66 generations calculated from its doubling time of 13.1 h, we observed that the growth rate under methanol doubled from 0.09 ± 0.02 OD_{545} day^{-1} in WT to 0.18 ± 0.01 OD_{545} day^{-1} (Figure 1b). The enhancement of autotrophic metabolism of methanol adapted strain was further evaluated by using H_2 as a reducing equivalent. Figure 1c−e display the autotrophic growth of methanol adapted and WT *S. ovata* under pressurized H_2:CO_2 (80%:20%) headspace and acetic acid concentrations measured by quantitative proton nuclear magnetic resonance (^{1}H-qNMR). The two strains exhibited similar growth during the initial incubation phase up to day 4 and became distinctive during the exponential phase (Figure 1c). The adapted strain had a shorter exponential doubling rate of 0.98 days than 1.40 days for the WT strain. The methanol adapted strain showed a 2.3-times faster exponential growth rate and a 1.3-times higher acetate production rate during the exponential phase, where nearly unlimited availability of substrates (H_2) to bacteria could be assumed. These results confirm that methanol adaptation leads to an enhanced rate of autotrophy in *S. ovata*.

S. ovata reduces two molecules of CO_2 via two separate branches of the WLP for biomass generation and energy conversion (Figure 2).[7,26] The carbonyl branch reduces CO_2 to CO, while the methyl branch reduces CO_2 to methyl group by several consecutive enzymatic steps.[7] Subsequently, the methyl group coupled with the CO from the carbonyl branch form Acetyl-CoA, which is converted to acetate by phosphotransacetylase and acetate kinase. In the methanol oxidation pathway (Figure 2a), the methyl group is first transferred to THF via methanol:THF methyltransferase to yield methyl-THF.[27] Then methyl-THF is fully oxidized to CO_2 in the methyl branch with the generation of reducing equivalents. Entering the carbonyl branch, CO_2 is condensed with the rest of methyl-THF and CoA to form acetyl-CoA. While oxidizing methanol or hydrogen, the two substrates offer a different set

https://doi.org/10.1021/acs.nanolett.2c01576
Nano Lett. XXXX, XXX, XXX−XXX

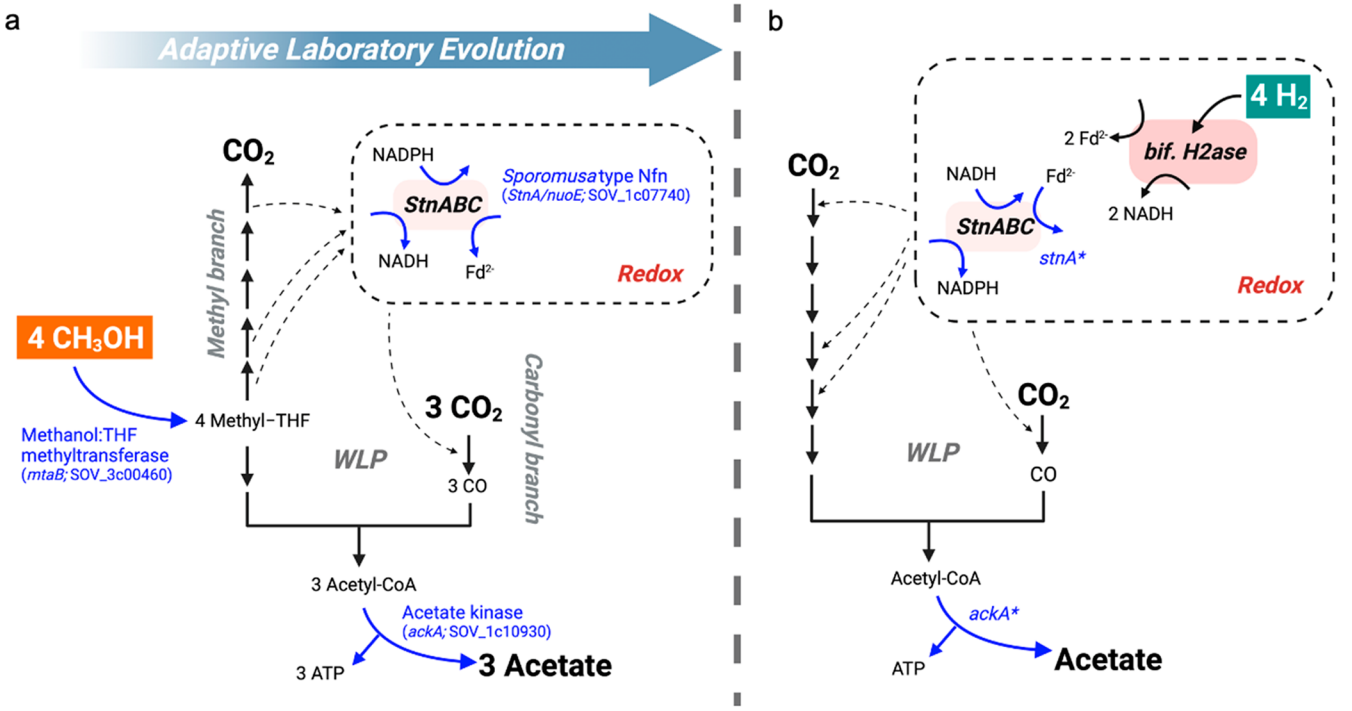

c

Region	Gene product	Amino acid position and change
ackA	Acetate kinase	748 A → G
mtaB	Subunit MtaB of Methanol:THF methyl transferase I	382 C → T
stnA/nuoE	Subunit StnA of *Sporomusa* type Nfn complex	394 G → A

Figure 2. Biochemistry of acetogenesis in *S. ovata* and mutations in the central metabolism. (a) Simplified methanol oxidation pathway of *S. ovata*. Mutated genes analyzed by the whole genome sequencing of adapted *S. ovata* are indicated in blue. (b) Simplified hydrogen oxidation pathway of *S. ovata*. The blue asterisks and arrows indicate the reactions catalyzed by the mutated gene products. The dashed boxes and arrows represent the oxidation or reduction reactions of biological electron carriers (e.g., NADH, NADPH). (c) Representative region of the genes containing the mutations in the central metabolism of *S. ovata*, the corresponding gene products, amino acid positions, and changes (see Table S1 for details). StnABC was recently proposed from ref 26. Fd, ferredoxin; bif. H_2ase, bifurcating hydrogenase.

of electron carriers (NADH, NADPH and ferredoxin) generated by the methyl-group oxidizing enzymes or bifurcating hydrogenase, respectively (Figure 2a,b). The recently proposed *Sporomusa*-type ferredoxin-dependent transhydrogenase (StnABC) allocates the specific electron carriers in the right amounts for the WLP.[26]

Whole genome sequencing (WGS) of adapted *S. ovata* was further used to correlate the mutant phenotypes to genomic changes relative to the WT genome sequence. Five single colonies of methanol adapted *S. ovata* were isolated and individually cultured in 2% methanol autotrophic media to evaluate the metabolic activity of single colonies. The whole genomes of the fastest-growing mutant, single colony 10 (Figure 1b), and WT strain were extracted and sequenced. As expected, based on the underlying physiology of *S. ovata* and the work of Tremblay et al., we observed mutations throughout the WLP (Figure 2a). While not identical single-nucleotide polymorphisms (SNPs), we observed five of SNPs in genes in which Tremblay et al. observed SNPs. These were the genes *ackA*, *mtaBC*, *nifB1*, and *dosC* (Table S1). For example, both our study and that of Tremblay et al. found SNPs in the gene *ackA* coding for the acetate kinase. Tremblay et al. confirmed that their observed SNP (R176Q) had an impact on the higher enzymatic activity of acetate kinase in the adapted strain, which aided in improving the overall efficiency of the WLP. In addition to the above SNPs, we observed some SNPs that were unique to this study. For example, an SNP in subunit A of the *Sporomusa*-type transhydrogenase, StnABC, was detected (Figure 2a). Overall, these SNP data support the adaptation of *S. ovata* to methanol and help elucidate the genetic basis of the observed phenotype.

Enhanced Bioelectrochemical CO_2 Fixation of Methanol Adapted *S. ovata* in Bacteria/Nanowire Hybrids. After the successful methanol adaptation of *S. ovata*, we examined the CO_2-reducing capability of methanol adapted and WT *S. ovata* in our close-packed nanowire/bacteria hybrid system. To compare the CO_2 reducing capabilities of the two different bacterial strains, we used a highly doped conductive p^+ Si NWs array as the cathode and platinum (Pt) wire as the anode. The SiNWs arrays were passivated by a 5 nm of TiO_2 as a protection layer and subsequently coated with Ni to facilitate the charge transfer from the cathode to the bacteria. Established inorganic phosphate-buffered media (pH 6.4) with trace vitamins as the only organic component was used as the electrolyte. *S. ovata* was inoculated into a catholyte (20% v/v at OD_{545} of 0.38) and cultured on the Si NWs array. The biohybrids were incubated on the cathodes for 3 days, close to the exponential doubling time of autotrophic growth of *S.*

https://doi.org/10.1021/acs.nanolett.2c01576
Nano Lett. XXXX, XXX, XXX−XXX

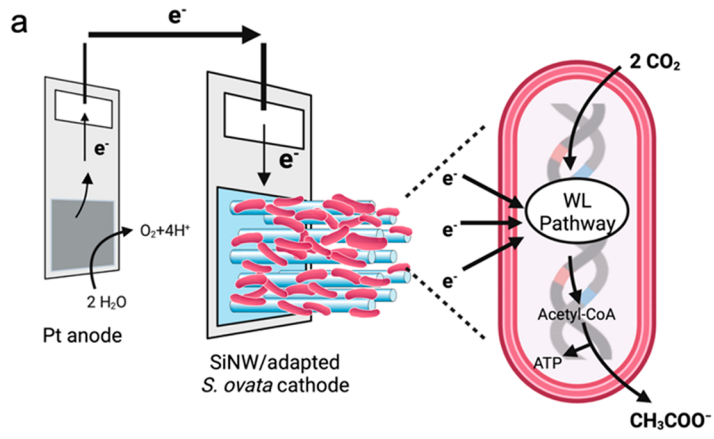

b

	TOR_{H2} (molecules s^{-1} $cell^{-1}$)	TOR_{e^-} (molecules s^{-1} $cell^{-1}$)
wild type	1.9×10^6	1.0×10^6
met-adapted	2.5×10^6	2.2×10^6

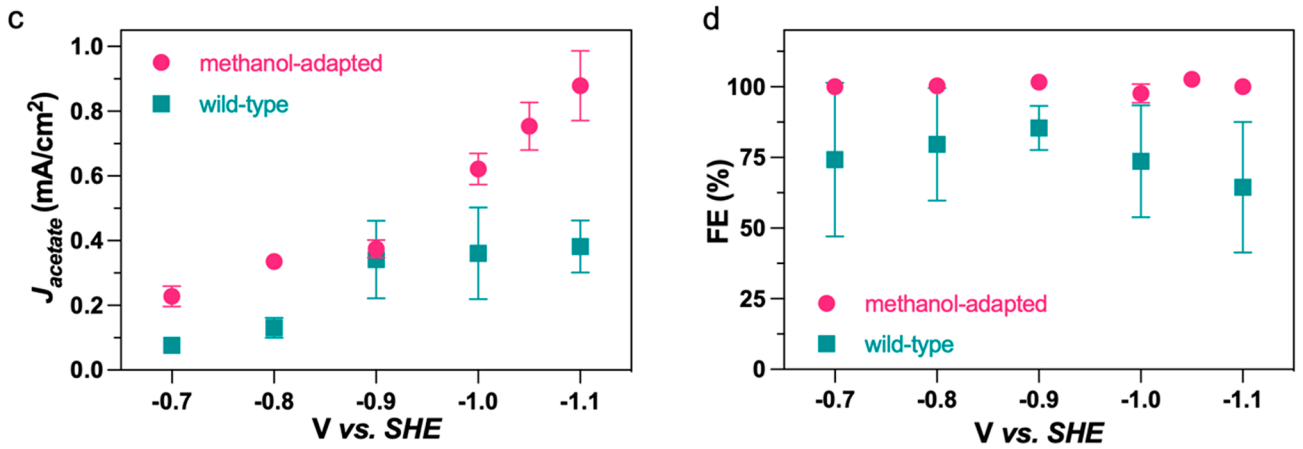

Figure 3. Electrochemical performance of nanowire/bacteria hybrids with methanol adapted *S. ovata* (red) and WT *S. ovata* (green). (a) Schematic illustration of the close-packed nanowire/bacteria hybrid system with SiNWs and the methanol adapted *S. ovata*. The electrons are transferred from the Si nanowire cathode to *S. ovata* and finally passed to the Wood−Ljungdahl pathway to produce acetate and ATP. (b) Turnover rates of acetate molecules under hydrogen (TOR_{H2}) and electron (TOR_{e^-}) by the methanol adapted *S. ovata* and WT *S. ovata*. Bias-dependent (c) $J_{acetate}$ and (d) $FE_{aceatate}$ of the close-packed nanowire/bacteria hybrids with the methanol adapted *S. ovata* and WT *S. ovata* using established inorganic phosphate-buffered media (pH 6.4). $J_{acetate}$ is defined as J_{total} multiplied by $FE_{aceatate}$ (see methods in Supporting Information). All error bars represent the mean ± s.d. (n = 3 biological independent samples).

ovata. Both *S. ovata* strains were densely packed in the nanowire array forming a close-packed hybrid structure supported by scanning electron microscopy (SEM) characterization (Figure S1). The calculated cell loading of adapted *S. ovata* within the nanowire array (per 4 μm^2 of projected area) from SEM images is slightly higher than that of WT *S. ovata*, ~13 and ~12, respectively, related to the faster cell growth of adapted *S. ovata* in autotrophic conditions. With this hybrid structure formed, we analyzed faradaic efficiencies of acetate ($FE_{acetate}$) and CO_2-reducing current density ($J_{acetate}$), which is a product of $FE_{acetate}$ and total current density (J_{total}), of each strain from chronoamperometry experiments at cathodic potentials from −0.7 to −1.1 V versus *SHE* (Figure 3). Compared to the pressurized hydrogen, the in situ resource of electrons, which serves as a reducing equivalent, is generated from the biased electrode with varying fluxes by controlling the potentials of the cathode. These gradually increasing fluxes of reducing equivalent can reveal the maximum flux of reducing equivalent that can be absorbed and integrated into the biohybrid systems as a final product of acetate. The flux of reducing equivalents and the rate of metabolism need to be well matched at the charge transfer interface. In Figure 3c, the adapted *S. ovata*/SiNW hybrid exhibited distinctively higher CO_2-reducing current densities at all potential regimes than did the WT strain. It achieved a 2.4-times higher maximum CO_2-reducing current density of 0.88 ± 0.1 mA/cm^2 at 1.1 V versus *SHE* compared to 0.38 ± 0.08 mA/cm^2 of the WT strain. The baseline data of the WT strain were consistent with our previous study of the close-packed hybrid system,[16] having overlapped error bars at all analyzed potentials (Figure S2). The previous study showed a 0.47 ± 0.07 mA/cm^2 of CO_2-reducing current density at −1.1 V versus *SHE*. Merely increasing the overpotentials could not stimulate the higher current densities, but the excessive electrons at the high overpotentials are consumed by the electrolyte near the electrode surface, turning the local environment inhospitable to the microorganisms to metabolize, as we observed previously.[16]

The maximum acetate turnover rate (TOR) of each system was calculated from the CO_2-reducing current density and the calculated cell loading density from SEM characterization (Figure 3b). The adapted *S. ovata* cell exhibits ~2.2×10^6 acetate molecules per second per cell (s^{-1} $cell^{-1}$), and the WT *S. ovata* cell shows ~1.0×10^6 acetate molecules s^{-1} $cell^{-1}$. Thus, the adapted strain has a higher capability to accept the faster flux of electron and convert it into acetate and it enables to achieve higher acetate current at the higher overpotential. On the other hand, the WT strain has a slower metabolism,

https://doi.org/10.1021/acs.nanolett.2c01576
Nano Lett. XXXX, XXX, XXX−XXX

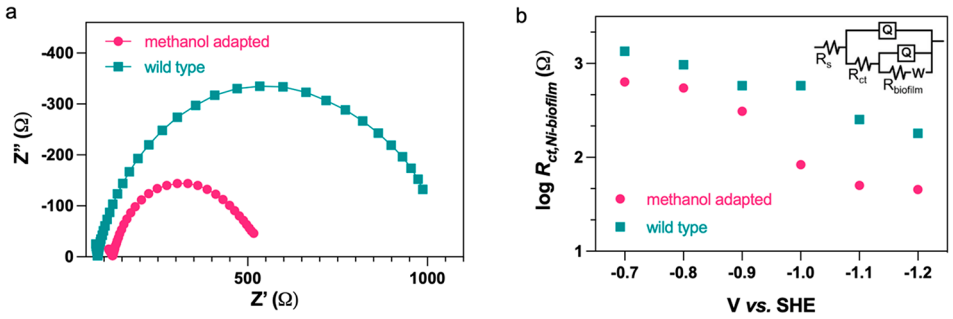

Figure 4. EIS characterization of Si nanowire/*S. ovata* hybrids system after chronoamperometry current uptake. (a) Representative Nyquist plots of the methanol adapted strain (red) and the WT strain (green) in established inorganic phosphate-buffered media at −0.9 V versus *SHE*. (b) Extracted charge transfer resistance (R_{ct}) values of the two systems using the methanol adapted *S. ovata* and WT *S. ovata*. An equivalent circuit model (inset in panel b) is built to mimic the electrochemical CO_2-reducing reaction of nanowire/bacteria hybrids.

and thus, below a certain potential, the flux of electrons is too high for them to uptake and the acetate current is just saturated depending on their inherent TOR capability. Moreover, considering that the inherent TOR of acetogenesis using hydrogen or methanol lies between $(0.3–6.9) \times 10^6$ acetate molecules s^{-1} $cell^{-1}$ (see Table S2 for details),[28] the TOR of the adapted *S. ovata*, 2.2×10^6 molecules s^{-1} $cell^{-1}$, suggests that the bacteria can continue to metabolize in our electrochemical reducing environment.

The enhanced CO_2-reduction rate, $J_{acetate}$, could be first confirmed by the higher mean faradaic efficiencies of adapted *S. ovata*, which were all over 90% with very small variances (Figure 3c). A faradaic efficiency at a certain potential formulates the ratio of electrons that are uptaken by *S. ovata* and then flow into the WLP, and thus, it reflects the susceptibility of collective CO_2-reducing capability of microbes at the corresponding flux of reducing equivalent. Noticeably at more negative potentials (at faster fluxes of reducing equivalents) from −1.0 to −1.1 V versus *SHE*, $FE_{acetate}$ of adapted strain was reproducibly maintained around 95%, unlike that of WT strain, which decreased from 90 to 40% and correspondingly lowered the mean CO_2-reducing rates. Excess unused electrons with high overpotentials not only decreases the faradic efficiency but also causes a toxic microenvironment caused by high pH near the cathode surface. The large variance is consistent with that of the previously reported $FE_{acetate}$ of WT strain.[16] The smaller variance of adapted strain reflects the basic principle of ALE of selecting fitter mutants among a microbial population of the wild-type strain and affirms a highly efficient CO_2-reducing metabolism of adapted *S. ovata* at a wide range of reducing equivalents fluxes. To further explore charge transfer kinetics, we performed in-depth electrochemical impedance spectroscopy (EIS) analysis of both systems.

Elucidation of Enhanced Charge Transfer Kinetics of Methanol Adapted *S. ovata* by Electrochemical Analytical Methods. To verify the charge transfer kinetics as well as to elucidate the enhancement of CO_2-reducing currents, we conducted the EIS characterization with frequencies ranging from 0.1 Hz to 1 MHz at cathodic potentials from −0.7 to −1.1 V versus *SHE*. The Nyquist plots from the two systems using the adapted *S. ovata* and WT *S. ovata* were obtained, and the resulting Nyquist plot (Figures 4a and S3) displays that the impedance (including $Z_{imaginary}$ and Z_{real}) changed with the strains used, as identified by the different radius of each Nyquist plot. To extract the quantitative impedance values and explain the correlation between the impedance and the applied potentials, an equivalent circuit model has been established (Figure 4b). In this model, two-electron pathways are connected in parallel, and the double-layer capacitance represents the nonfaradic process. The faradic process is governed by the electron transfer pathway from the top-coated Ni thin film to bacteria within the biofilm. The charge transfer resistance, catalyst resistance, and catalyst capacitance are annotated with R_{ct}, $R_{bacteria}$ and $C_{bacteria}$, respectively. On the basis of this equivalent circuit model, the charge transfer resistance is extracted as a function of the applied electrochemical potential (Figure 4b and Table S3). Distinctively, the R_{ct} of adapted bacteria is smaller than that of WT bacteria at all overpotential regimes, consistent with the higher CO_2-reducing current densities and total current densities of the adapted *S. ovata* system. Provided that the charge transfer resistance is crucial for the kinetics at the electrode/electrolyte interface, this quantitative difference between two strains obtained from the impedance spectroscopy further supports that enhancing the CO_2-fixing metabolic activity of the whole-cell catalysts can promote the faster charge transfer from the electrode to bacteria.

The lower charge transfer resistance could merely arise from the increase of interfacial area between bacteria and the electrode.[29−31] SEM characterization revealed that both bacteria strains maintained a close-packed hybrid structure for electrolytes and slightly higher cell density of adapted strain around nanowires as previously discussed (Figure S1). To quantitatively obtain the interfacial area of cell binding on our electrode, we conducted the impedance-based bacterial detection method proposed by Ariel et al.[32] Here, a high concentration of methyl viologen is added into the media to decrease the charge transfer resistance of the electrode at its open circuit potential, and electrons are mainly transferred to methyl viologen as shown in the redox peak from the cyclic voltammetry plots (Figure S4a,b). The similar charge transfer resistance from the two systems (Figure S4c) suggests a similar degree of cell binding in each system, which is consistent with the previous results of SEM characterization. This implies that the lower charge transfer resistance should arise from another factor in addition to the increased cell loading, such as the fast consumption of intermediate species, as supported by the higher turnover rate of the adapted strain. Future studies would be required to directly prove such enhanced charge transfer kinetics of adapted *S. ovata*.

Altogether, our results demonstrate a distinctive way to improve the efficiency of biohybrid CO_2 fixation by introducing methanol adaptation of *S. ovata* and enhancing

https://doi.org/10.1021/acs.nanolett.2c01576
Nano Lett. XXXX, XXX, XXX−XXX

autotrophic metabolism by ALE. The key to success was that the inherent TOR of the strain should match the high flux of reducing equivalents generated from the high-surface-area nanowire. We namely show that the enhancement of autotrophic metabolism under methanol was reproducibly observed under hydrogen and electron as a growth substrate. The synergetic combination of the adapted strain and Si NWs ultimately enhances the CO_2 reducing rate in our model system 2.4-fold higher as compared to the system using wild-type strain. Besides high catalytic efficiency, the methanol adapted strain also can offer the hallmarks of the biology: self-replication and self-repair. This strategy could further improve the CO_2 conversion rate and solar-to-chemical efficiency in photoelectrochemical systems.[33−35]

■ ASSOCIATED CONTENT

Supporting Information

The Supporting Information is available free of charge at https://pubs.acs.org/doi/10.1021/acs.nanolett.2c01576.

Description of experimental details and additional characterization data; figures of SEM images, chronoamperometry characterization, EIS characterization, cell binding characterization; tables of whole genome sequencing results, inherent TOR values, EIS raw data (PDF)

■ AUTHOR INFORMATION

Corresponding Author

Peidong Yang − *Department of Materials Science and Engineering, University of California, Berkeley, California 94720, United States; Center for the Utilization of Biological Engineering in Space (CUBES), Berkeley, California 94720, United States; Department of Chemistry, University of California, Berkeley, California 94720, United States; Materials Sciences Division, Lawrence Berkeley National Laboratory, Berkeley, California 94720, United States; Kavli Energy Nanoscience Institute, Berkeley, California 94720, United States;* orcid.org/0000-0003-4799-1684; Email: p_yang@berkeley.edu

Authors

Jimin Kim − *Department of Materials Science and Engineering, University of California, Berkeley, California 94720, United States; Center for the Utilization of Biological Engineering in Space (CUBES), Berkeley, California 94720, United States*

Stefano Cestellos-Blanco − *Department of Materials Science and Engineering, University of California, Berkeley, California 94720, United States; Center for the Utilization of Biological Engineering in Space (CUBES), Berkeley, California 94720, United States*

Yue-xiao Shen − *Department of Chemistry, University of California, Berkeley, California 94720, United States; Department of Civil, Environmental and Construction Engineering, Texas Tech University, Lubbock, Texas 79409, United States*

Rong Cai − *Department of Chemistry, University of California, Berkeley, California 94720, United States*

Complete contact information is available at: https://pubs.acs.org/10.1021/acs.nanolett.2c01576

Author Contributions

J.K. and P.Y. designed the experiments. S.C.-B. and J.K. fabricated the silicon nanowire electrodes. J.K., S.C.-B., Y.-x.S., and R.C. performed the bacteria culturing and incubation. J.K., S.C.-B., Y.-x.S., and R.C. performed the electrochemical experiments. J.K. performed the genome sequencing and SNP analysis. J.K. and P.Y. cowrote the paper. All authors discussed the results and revised the manuscript.

Notes

The authors declare no competing financial interest.

■ ACKNOWLEDGMENTS

This work was supported by the National Aeronautics and Space Administration (NASA) under Grant No. NNX17AJ31G. We thank the Marvell Nanofabrication Laboratory for use of their facilities. We thank the NMR facility of the College of Chemistry, University of California, Berkeley. We thank Dr. Adam Paul Arkin and Dr. Jacob Hilzinger from Department of Bioengineering, University of California, Berkeley, for the helpful discussions about whole genome sequencing and SNP analysis. J.K. acknowledges the fellowship support from Kwanjeong educational foundation. S.C.-B. thanks the Philomathia foundation.

■ REFERENCES

(1) Jordaan, S. M.; Wang, C. Electrocatalytic Conversion of Carbon Dioxide for the Paris Goals. *Nat. Catal.* **2021**, *4* (11), 915−920.

(2) Cestellos-Blanco, S.; Zhang, H.; Kim, J. M.; Shen, Y. x.; Yang, P. Photosynthetic Semiconductor Biohybrids for Solar-Driven Biocatalysis. *Nat. Catal.* **2020**, *3*, 245−255.

(3) Zhang, H.; Liu, H.; Tian, Z.; Lu, D.; Yu, Y.; Cestellos-Blanco, S.; Sakimoto, K. K.; Yang, P. Bacteria Photosensitized by Intracellular Gold Nanoclusters for Solar Fuel Production. *Nat. Nanotechnol.* **2018**, *13* (10), 900−905.

(4) Birdja, Y. Y.; Pérez-Gallent, E.; Figueiredo, M. C.; Göttle, A. J.; Calle-Vallejo, F.; Koper, M. T. M. Advances and Challenges in Understanding the Electrocatalytic Conversion of Carbon Dioxide to Fuels. *Nat. Energy* **2019**, *4* (9), 732−745.

(5) Fan, L.; Xia, C.; Yang, F.; Wang, J.; Wang, H.; Lu, Y. Strategies in Catalysts and Electrolyzer Design for Electrochemical CO2 Reduction toward C2+ Products. *Sci. Adv.* **2020**, *6* (8), 1−18.

(6) Hong, D.; Lee, H.; Ko, E. H.; Lee, J.; Cho, H.; Park, M.; Yang, S. H.; Choi, I. S. Organic/Inorganic Double-Layered Shells for Multiple Cytoprotection of Individual Living Cells. *Chem. Sci.* **2015**, *6* (1), 203−208.

(7) Schuchmann, K.; Müller, V. Autotrophy at the Thermodynamic Limit of Life: A Model for Energy Conservation in Acetogenic Bacteria. *Nat. Rev. Microbiol.* **2014**, *12* (12), 809−821.

(8) Song, Y.; Lee, J. S.; Shin, J.; Lee, G. M.; Jin, S.; Kang, S.; Lee, J. K.; Kim, D. R.; Lee, E. Y.; Kim, S. C.; Cho, S.; Kim, D.; Cho, B. K. Functional Cooperation of the Glycine Synthasereductase and Wood-Ljungdahl Pathways for Autotrophic Growth of Clostridium Drakei. *Proc. Natl. Acad. Sci. U. S. A.* **2020**, *117* (13), 7516−7523.

(9) Nevin, K. P.; Hensley, S. A.; Franks, A. E.; Summers, Z. M.; Ou, J.; Woodard, T. L.; Snoeyenbos-West, O. L.; Lovley, D. R. Electrosynthesis of Organic Compounds from Carbon Dioxide Is Catalyzed by a Diversity of Acetogenic Microorganisms. *Appl. Environ. Microbiol.* **2011**, *77* (9), 2882−2886.

(10) Lovley, D. R.; Nevin, K. P. Electrobiocommodities: Powering Microbial Production of Fuels and Commodity Chemicals from Carbon Dioxide with Electricity. *Curr. Opin. Biotechnol.* **2013**, *24* (3), 385−390.

(11) Picard, A.; Gartman, A.; Girguis, P. R. What Do We Really Know about the Role of Microorganisms in Iron Sulfide Mineral Formation? *Front. Earth Sci.* **2016**, *4*, 68 DOI: 10.3389/feart.2016.00068.

(12) LaBelle, E. V.; May, H. D. Energy Efficiency and Productivity Enhancement of Microbial Electrosynthesis of Acetate. *Front. Microbiol.* **2017**, *8* (MAY), 1−9.
(13) Ameen, F.; Alshehri, W. A.; Nadhari, S. Al. Effect of Electroactive Biofilm Formation on Acetic Acid Production in Anaerobic Sludge Driven Microbial Electrosynthesis. *ACS Sustain. Chem. Eng.* **2020**, *8* (1), 311−318.
(14) Perona-Vico, E.; Feliu-Paradeda, L.; Puig, S.; Bañeras, L. Bacteria Coated Cathodes as an In-Situ Hydrogen Evolving Platform for Microbial Electrosynthesis. *Sci. Rep.* **2020**, *10* (1), 1−11.
(15) Liu, C.; Gallagher, J. J.; Sakimoto, K. K.; Nichols, E. M.; Chang, C. J.; Chang, M. C. Y.; Yang, P. Nanowire-Bacteria Hybrids for Unassisted Solar Carbon Dioxide Fixation to Value-Added Chemicals. *Nano Lett.* **2015**, *15* (5), 3634−3639.
(16) Su, Y.; Cestellos-Blanco, S.; Kim, J. M.; Shen, Y. x.; Kong, Q.; Lu, D.; Liu, C.; Zhang, H.; Cao, Y.; Yang, P. Close-Packed Nanowire-Bacteria Hybrids for Efficient Solar-Driven CO2 Fixation. *Joule* **2020**, *4* (4), 800−811.
(17) Kim, D.; Sakimoto, K. K.; Hong, D.; Yang, P. Artificial Photosynthesis for Sustainable Fuel and Chemical Production. *Angew. Chemie - Int. Ed.* **2015**, *54* (11), 3259−3266.
(18) Dinh, C. T.; Burdyny, T.; Kibria, G.; Seifitokaldani, A.; Gabardo, C. M.; García De Arquer, F. P.; Kiani, A.; Edwards, J. P.; De Luna, P.; Bushuyev, O. S.; Zou, C.; Quintero-Bermudez, R.; Pang, Y.; Sinton, D.; Sargent, E. H. CO2 Electroreduction to Ethylene via Hydroxide-Mediated Copper Catalysis at an Abrupt Interface. *Science (80-.)* **2018**, *360* (6390), 783−787.
(19) Li, Y. C.; Wang, Z.; Yuan, T.; Nam, D. H.; Luo, M.; Wicks, J.; Chen, B.; Li, J.; Li, F.; De Arquer, F. P. G.; Wang, Y.; Dinh, C. T.; Voznyy, O.; Sinton, D.; Sargent, E. H. Binding Site Diversity Promotes CO2 Electroreduction to Ethanol. *J. Am. Chem. Soc.* **2019**, *141* (21), 8584−8591.
(20) Abel, A. J.; Clark, D. S. A Comprehensive Modeling Analysis of Formate-Mediated Microbial Electrosynthesis**. *ChemSusChem* **2021**, *14* (1), 344−355.
(21) Sahoo, P. C.; Pant, D.; Kumar, M.; Puri, S. K.; Ramakumar, S. S. V. Material−Microbe Interfaces for Solar-Driven CO2 Bioelectrosynthesis. *Trends Biotechnol* **2020**, *38* (11), 1245−1261.
(22) Weliwatte, N. S.; Minteer, S. D. Photo-Bioelectrocatalytic CO2 Reduction for a Circular Energy Landscape. *Joule* **2021**, *5* (10), 2564−2592.
(23) Tremblay, P. L.; Höglund, D.; Koza, A.; Bonde, I.; Zhang, T. Adaptation of the Autotrophic Acetogen Sporomusa Ovata to Methanol Accelerates the Conversion of CO2 to Organic Products. *Sci. Rep.* **2015**, *5*, 1−11.
(24) Gleizer, S.; Ben-Nissan, R.; Bar-On, Y. M.; Antonovsky, N.; Noor, E.; Zohar, Y.; Jona, G.; Krieger, E.; Shamshoum, M.; Bar-Even, A.; Milo, R. Conversion of Escherichia Coli to Generate All Biomass Carbon from CO2. *Cell* **2019**, *179* (6), 1255−1263.e12.
(25) Portnoy, V. A.; Bezdan, D.; Zengler, K. Adaptive Laboratory Evolution-Harnessing the Power of Biology for Metabolic Engineering. *Curr. Opin. Biotechnol.* **2011**, *22* (4), 590−594.
(26) Kremp, F.; Roth, J.; Müller, V. The Sporomusa Type Nfn Is a Novel Type of Electron-Bifurcating Transhydrogenase That Links the Redox Pools in Acetogenic Bacteria. *Sci. Rep.* **2020**, *10* (1), 1−14.
(27) Kremp, F.; Müller, V. Methanol and Methyl Group Conversion in Acetogenic Bacteria: Biochemistry, Physiology and Application. *FEMS Microbiol. Rev.* **2021**, *45* (2), 1−22.
(28) Claassens, N. J.; Cotton, C. A. R.; Kopljar, D.; Bar-Even, A. Making Quantitative Sense of Electromicrobial Production. *Nat. Catal.* **2019**, *2* (5), 437−447.
(29) Kretzschmar, J.; Harnisch, F. Electrochemical Impedance Spectroscopy on Biofilm Electrodes − Conclusive or Euphonious? *Curr. Opin. Electrochem.* **2021**, *29* (April), 100757.
(30) Mccuskey, S. R.; Su, Y.; Leifert, D.; Moreland, A. S.; Bazan, G. C. Living Bioelectrochemical Composites. *Adv. Mater.* **2020**, *32* (24), 1908178.
(31) Luo, H.; Qi, J.; Zhou, M.; Liu, G.; Lu, Y.; Zhang, R.; Zeng, C. Enhanced Electron Transfer on Microbial Electrosynthesis Biocathode by Polypyrrole-Coated Acetogens. *Bioresour. Technol.* **2020**, *309* (April), 123322.
(32) Furst, A. L.; Francis, M. B. Impedance-Based Detection of Bacteria. *Chem. Rev.* **2019**, *119* (1), 700−726.
(33) Deng, X.; Dohmae, N.; Kaksonen, A. H.; Okamoto, A. Biogenic Iron Sulfide Nanoparticles to Enable Extracellular Electron Uptake in Sulfate-Reducing Bacteria. *Angew. Chemie - Int. Ed.* **2020**, *59* (15), 5995−5999.
(34) Liu, C.; Gallagher, J. J.; Sakimoto, K. K.; Nichols, E. M.; Chang, C. J.; Chang, M. C. Y.; Yang, P. Nanowire−Bacteria Hybrids for Unassisted Solar Carbon Dioxide Fixation. *Nano Lett.* **2015**, *15* (5), 3634−3639.
(35) Kong, X.; Gai, P.; Li, F. Biohybrid Cells for Photoelectrochemical Conversion Based on the HCOO–CO2Circulation Approach. *ACS Appl. Bio Mater.* **2020**, *3* (11), 8069−8074.

https://doi.org/10.1021/acs.nanolett.2c01576
Nano Lett. XXXX, XXX, XXX−XXX